NOSE PRESSURE FLUCTUATIONS FOR A FINITE-THICKNESS SYMMETRIC BODY PENETRATING A SINUSOIDAL TRANSVERSE VELOCITY FIELD

Frank Lane

KLD Associates, Incorporated

Prepared for:

Advanced Research Projects Agency
Army Missile Command

July 1974

KLD TR-23

Semi-Annual Report No. 1
Period Ending 16 July 1974

NOSE PRESSURE FLUCTUATIONS FOR A FINITE-THICKNESS SYMMETRIC BODY PENETRATING A SINUSOIDAL TRANSVERSE VELOCITY FIELD

by

Frank Lane

SPONSORED BY:

Advanced Research Projects Agency
Department of Defense
ARPA Order No. 2126

MONITORED BY:

U. S. Army Missile Command
Redstone Arsenal, Alabama 35809
Contract No. DAAH01-74-C-0480

Amount of Contract:	$67,452.00
Effective Date of Contract:	Jan. 16, 1974
Contract Expiration Date:	Jan. 15, 1975
Project Scientist and Phone:	Dr. Frank Lane 516-549-9803

Prepared by

KLD Associates, Inc.
7 High Street
Huntington, New York 11743

July 1974

TABLE OF CONTENTS

ABSTRACT

The effects of the transverse component of velocity fluctuations on nominal stagnation point (NSP) pressure fluctuations are analyzed for a finite-thickness symmetric body penetrating into a turbulent flow. The analysis is idealized to the case of a two-dimensional symmetric airfoil-like profile. Considerations are limited to fluctuation scales which are large relative to airfoil thickness but not necessarily large relative to airfoil chord. A single wave-number component of the turbulence is analyzed, permitting synthesis for any desired wave-number spectrum, within the above-mentioned limitation on minimum scale size or maximum wave number.

The results are given in analytical form for transverse-velocity-fluctuation induced pressure fluctuation at the NSP. These results are then compared to a measure of axial-velocity induced fluctuations. The important parameters in this comparison are shown to be $\frac{\text{fluctuation scale}}{\text{nose radius}}$ and $\frac{\text{fluctuation velocity}}{\text{penetration velocity}}$. When the product of these ratios is $\left\{\begin{matrix}\ll \\ \gtrsim\end{matrix}\right\}$ 20 the transverse-velocity fluctuation v' $\left\{\begin{matrix}\text{is dominated by} \\ \text{is of the same effectiveness as} \\ \text{dominates}\end{matrix}\right\}$ the axial-velocity fluctuation u' in inducing pressure fluctuations p' at the NSP. For the case where the axial component dominates, existing references give the relation between u' and p' adequately. For the case where the transverse component v' dominates, the present report gives the relation between v' and p'. The intermediate regime requires a combination of the two contributions.

I. INTRODUCTION

This report deals with certain aspects of the general problem of relating the pressure fluctuations sensed at the nose of a symmetric body to the velocity fluctuations present in the fluid medium through which the body is penetrating. Considerations are limited to low-speed or incompressible flows. The experimental work of Bearman,[1] together with the analytical background cited therein, forms a basis for relating the two aforementioned fluctuation quantities when the scales of the encountered fluctuations are much smaller than the body length in the streamwise direction.

Here, however, we are interested specifically in situations for which the encountered fluctuation spectrum (in wave-number space) has significant energy in the wave-number regime corresponding to the chord-length of the penetrating body. In the small-scale regime considered by Bearman, the pressure fluctuations could be related roughly to the axial component (or streamwise component) of velocity fluctuations. It is not clear that this is still true when the encountered fluctuation scales become as large as the chord length of the penetrating body, since the transverse velocity fluctuations then start to affect the nose-region flow via the nonsteady circulation induced about the body.

Thus the objective of the present report is to estimate the significance of the transverse component of encountered velocity fluctuations upon pressure fluctuations sensed at the nominal stagnation point (NSP) of a symmetric airfoil-like profile traversing a turbulent fluid medium. More specifically, the intent is to determine when, if ever, the transverse fluctuation component, through the mechanism of inducing stagnation-point meandering, can become as important as the axial fluctuation component in affecting the fluctuation pressure sensed at the NSP.

In view of the complexity of a completely detailed analysis, the approach to be taken is as follows: A symmetric two-dimensional wing moving at velocity U_o at zero nominal incidence, is presumed to penetrate a sinusoidal gust of transverse velocity $v(x-U_o t)$ in wing-fixed coordinates. That is, the velocity fluctuation is assumed to be essentially stationary in fluid coordinates or to be convected in at free-stream velocity U_o in wing-fixed coordinates. This is the classical 2-D sinusoidal gust-entry problem. The convection assumption is equivalent to ignoring any mean flow in the ambient fluctuating field.

The present analysis goes beyond the classical gust-entry problem insofar as the classical problem treats a zero-thickness flat plate, whereas we must not only include thickness but, most important, we must examine the very nose point where the classical theory becomes singular. Thus we must somehow supplement or alter the classical gust entry problem to permit detailed examination of nose-region pressure fluctuations for an actual finite-thickness profile.

The thick-wing corrections to thin-airfoil theory that are available in the literature (to the present author's knowledge) are limited to symmetric flow over symmetric profiles or to steady asymmetric flow (cambered profiles or profiles at nonzero incidence). [6,7] The present requirement is for nonsteady, nonsymmetric flow, and a treatment will be developed herein specifically for this purpose. The results are then compared with the steady, asymmetric, thick-wing results of Reference 7.

An approximate measure of the NSP fluctuation pressure due to the axial component of velocity fluctuation will be provided as a basis for comparison of the relative importance of the transverse-component effect. We will be interested in wavelengths λ_o of encountered fluctuations of the order of the chord length (c) of the penetrating airfoil. The thickness-to-chord ratio of the airfoil is small of the order of (ε) (this will be defined more carefully later), and it will be assumed that λ_o is considerably larger than εc, i.e., that ε is small and that the fluctuation scales encountered are large compared to airfoil thickness. This is a condition of definite physical interest.

In view of the fact that we are interested only in details in the wing nose region, we shall be content with performing the detailed analysis for a classical symmetric Joukowski profile. Then, at the end of Section VII, it is shown how to extend the results to more general symmetric profiles by relating the present results to those of Lighthill's theory for rendering approximate solutions uniformly valid.

Intuitively, since thin-airfoil gust-entry theory leads to a pressure singularity at the wing leading edge and fails altogether to provide for a stagnation point, we expect that the effect of transverse velocity fluctuations on stagnation-point oscillation and consequent pressure fluctuation at NSP will become more severe as the airfoil thickness-to-chord ratio (order ε) decreases. This will turn out to be true. We also expect, intuitively that the effect will depend upon

the ratio of chord to encountered wavelength (c/λ_o), and this will be true as well. What our intuition cannot predict is the strength or power to which these effects enter nor the appropriate coefficients, and these will emerge directly.

Summarizing the assumptions to be invoked, we list them here concisely for convenience :

Two-dimensional approximation

Symmetric Joukowski profile at zero incidence. It is then shown, at the end of Section VII how to generalize to more arbitrary symmetric profiles.

Zero mean velocity in "turbulent" flow encountered.

Spatially sinusoidal transverse velocity fluctuations encountered (these can, of course, be synthesized into a full spectrum of all wavelengths, subject to the following restriction).

Encountered wavelengths λ_o large compared to airfoil thickness but not necessarily large compared to chord length.

II. ACCOUNTING FOR THICKNESS BY MAPPING

We take account of airfoil thickness by performing a sequence of two conformal mappings from the physical (z) plane. These are illustrated schematically in Figure 1. First we map from z, where we have our physical Joukowski symmetric profile, to the intermediate ζ-plane wherein the airfoil maps to the (outer) eccentric circle. The mapping is given by

$$z = \frac{1}{2}\left(\zeta + \frac{\ell^2}{\zeta}\right) \tag{2-1}$$

and the aforementioned circle in the ζ-plane can be given, in terms of the angle parameter θ, as

$$\zeta_c = -\ell\epsilon + \ell(1+\epsilon)e^{i\theta} \tag{2-2}$$

Note that angle θ is defined with respect to the displaced center $(-\ell\epsilon, o)$ and not the origin in the ζ plane. As indicated on the figure, the trailing edge of the physical airfoil in the z-plane is located at

$$z = (\ell, o) \tag{2-3}$$

and the leading edge is approximately located at

$$\begin{aligned} z &= (-\ell(1+2\epsilon^2), o) \\ &\cong (-\ell, o) \end{aligned} \tag{2-4}$$

for small ϵ.

The points on the physical profile corresponding to

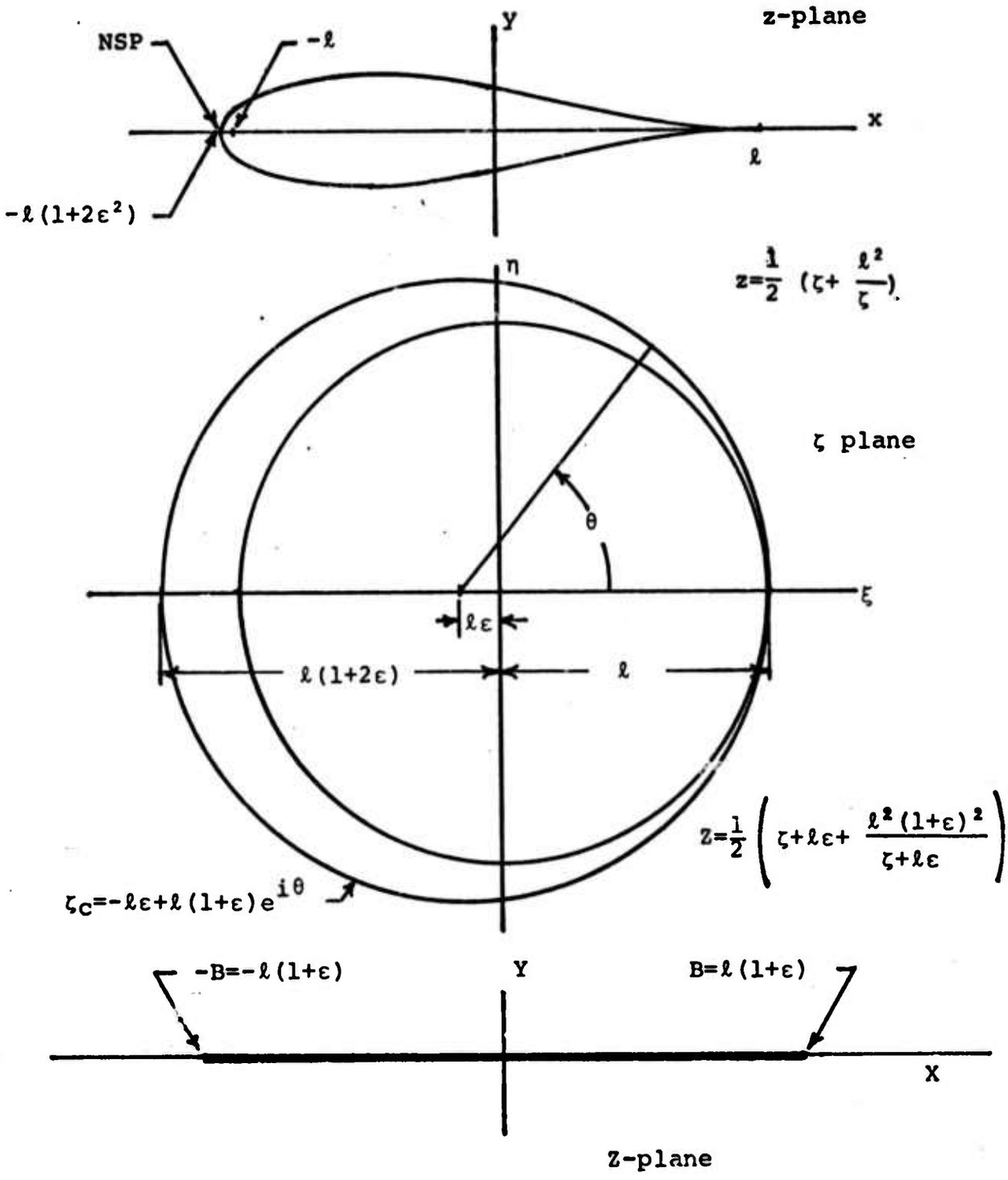

Figure 1

MAPPINGS

$\theta = \pm \pi/2$ are given by

$$z^{\pm} \cong -l\epsilon \pm il\epsilon \qquad (2\text{-}5)$$

indicating a local thickness of $2l\epsilon$. However, the maximum z-plane thickness occurs (Ref. 1) for $\cos\theta = -1/2$ and is larger by a factor of $3\sqrt{3}/4$. Thus the thickness-to-length ratio is given closely by

$$\frac{2l\epsilon \times \frac{3\sqrt{3}}{4}}{2l} = \frac{3\sqrt{3}}{4}\,\epsilon \cong 1.3\,\epsilon \qquad (2\text{-}6)$$

Thus ϵ has the physical significance

$$\epsilon \cong \frac{1}{1.3} \quad \frac{\text{thickness}}{\text{chord}} \qquad (2\text{-}7)$$

$$\cong 0.77 \quad \frac{\text{thickness}}{\text{chord}}$$

The second mapping, from ζ to Z, is given by

$$Z = \frac{1}{2}\left(\zeta + l\epsilon + \frac{l^2(1+\epsilon)^2}{\zeta + l\epsilon}\right) \qquad (2\text{-}8)$$

and maps the contour ζ_c to a slit of zero thickness in the Z plane with leading edge at (-B,0) and trailing edge at (+B,0).

Here

$$B = l(1+\epsilon) \qquad (2\text{-}9)$$

is the semichord of the Z-plane slit.

The motivation for this double-mapping is as follows: We can do the gust entry problem for the slit (in the Z plane) by classical techniques. Then by going back through the mapping from Z to ζ we just cancel out the expected Z-plane leading-edge singularity. Then by mapping from ζ to the physical z-plane, we leave the singularity of the (ζ to z) transformation inside the physical airfoil and retrieve the flow in the physical plane. This sequence permits us to utilize classical sinusoidal gust-entry theory for flat plates, and despite the leading-edge pressure singularity occurring therein, transform the result to a finite-thickness profile and compute the leading edge pressure fluctuation on this profile.

The requirement that the fluctuation scale be large with respect to the airfoil thickness is necessitated by our classical gust-entry treatment of the Z-plane flat-plate airfoil. Only under this scale-size assumption is it legal to assume that the encountered transverse velocity is the same on upper and lower surfaces of the physical airfoil at the same chordwise point, x. This, in turn, is implicit in the classical treatment of the Z-plane slit where the transverse gust to be counteracted by a potential flow is identical on upper and lower surfaces of the slit at the same value of X.

III. FLOWS IN THE VARIOUS PLANES

Defining the complex potential function by $F(z)=F(\zeta)=F(Z)$ at corresponding points, where

$$F = \varphi + i\psi \tag{3-1}$$

and where ϕ is the velocity potential and ψ is the stream function, we have for the basic (zero-disturbance) flow in the ζ-plane,

$$F_o(\zeta) = \frac{U_o}{2}\left(\zeta + \ell\epsilon + \frac{\ell^2(1+\epsilon)^2}{\zeta+\ell\epsilon}\right) \tag{3-2}$$

In the Z plane, this is simply

$$F_o(Z) = U_o Z \tag{3-3}$$

which is the purely uniform flow in the positive X direction, as it should be.

Inverting Eq. (2-1) for ζ, we find

$$\zeta = z + \sqrt{z^2-\ell^2} \tag{3-4}$$

This gives, for the basic flow in the z plane,

$$F_o(z) = \frac{U_o}{2}\left(z + \ell\epsilon + \sqrt{z^2-\ell^2} + \frac{\ell^2(1+\epsilon)^2}{z+\ell\epsilon+\sqrt{z^2-\ell^2}}\right) \tag{3-5}$$

In the far field (|z|large) this approaches

$$F_o(z) \sim U_o z \qquad \text{(uniform flow)} \qquad (3\text{-}6)$$

as it should. $F_o(z)$ is the complex potential for uniform flow of velocity U_o in the positive x direction over the Joukowski profile of Figure 1, i.e., in the physical plane.

On the profile $\zeta=\zeta_c$ in the ζ-plane,

$$\left.\begin{aligned} F_o(\zeta_c) &= \frac{U_o}{2}\left(\ell(1+\epsilon)e^{i\theta} + \frac{\ell^2(1+\epsilon)^2}{\ell(1+\epsilon)e^{i\theta}}\right) \\ &= U_o\,\ell(1+\epsilon)\cos\theta = \text{pure real} \end{aligned}\right\} \qquad (3\text{-}7)$$

so that $\psi=o$, and the profile is the zero-streamline in all three planes.

The complex velocity

$w = u - iv$ is given, in each plane by

$$w(z) = \frac{dF(z)}{dz}$$

$$w(\zeta) = \frac{dF}{d\zeta}$$

$$w(Z) = \frac{dF}{dZ} \qquad (3\text{-}8)$$

We can therefore find the z (physical)-plane flow from the Z-plane flow using the relation

$$\left.\begin{aligned} w(z) &= w(Z)\,\frac{\frac{dZ}{d\zeta}}{\frac{dz}{d\zeta}} \\ &= w(Z)\,\frac{\left(1 - \frac{\ell^2(1+\epsilon)^2}{(\zeta+\ell\epsilon)^2}\right)}{\left(1 - \frac{\ell^2}{\zeta^2}\right)} \end{aligned}\right\} \qquad (3\text{-}9)$$

At the leading edge (corresponding to $\zeta=-\ell(1+2\epsilon)$ the denominator $dz/d\zeta$ is regular, nonzero, but the numerator $dZ/d\zeta$ vanishes. However, it will turn out that our required nonsteady flow in the Z plane will approach infinity at the leading edge ($Z\to(-B,0)$) in just such a way as to balance the vanishing of $dZ/d\zeta$, and thereby contribute the bounded, nonzero velocity at the NSP in the physical plane.

Now in the inflow in the Z-plane we superimpose on the uniform U_o-flow a frozen sinusoidal transverse gust whose form, on the X_{axis}, is

$$v = v_o \cos(\omega_o t - k_o X) \qquad (3\text{-}10)$$

$$v_o < \epsilon\, U_o$$

with

$$k_o = \frac{2\pi}{\lambda_o} = \frac{\omega_o}{U_o} \qquad (3\text{-}11)$$

Since, $|Z|$, $\frac{|\zeta|}{2}$, $|z|$ all $\to \infty$ together and, for large negative X,

$$x \sim X \tag{3-12}$$

(see Eqs. (2-1) and (2-8),

and since the mappings are conformal (angle-preserving), therefore this sinusoidal transverse gust must correspond or map to the same transverse inflow in the field far upstream of the wing in the physical z-plane. We must then find that potential flow which exactly counteracts the gust (Eq. (3-10)) on the slit airfoil in the Z-plane. This flow when mapped to the z-plane, will then leave the physical airfoil a streamline and hence provide the proper flow in the physical plane, when the (far upstream) inflow in the physical plane is as required; namely the uniform flow U_o plus the frozen transverse sinusoidal gust. The solution for the counteracting potential flow in the Z plane is the classical thin-airfoil sinusoidal gust entry problem, except that we need the vorticity or pressure-jump distribution in detail, whereas the usual derivations are content with integrals for lift and moment.

IV. PRESSURE AT NSP IN THE PHYSICAL PLANE

After we have found the required counteracting potential flow we must then utilize it to construct the pressure at the nose (NSP) of the physical airfoil. For this we use the nonsteady Bernoulli equation

$$\left[\frac{\partial\varphi}{\partial t} + p + \rho_o q^2/2\right]_\infty = p + \rho_o q^2/2 + \rho_o \frac{\partial\varphi}{\partial t} \qquad (4\text{-}1)$$

Now, as noted (Eq. (3-10)) in the preceding section,

$$v_o \ll U_o \qquad \text{or} \qquad v_o < \epsilon U_o$$

so that the left side of (4-1) is essentially equal to

$$\left(p_\infty + \rho_o U_o^2/2 + \frac{\partial\varphi}{\partial t}\bigg|_\infty\right) + O(U_o^2 \epsilon^2 \rho_o) \; . \qquad (4\text{-}2)$$

On the right-hand side of Eq. (4-1) we need the velocity $q = |u+iv|$ which consists of superimposed contributions from the undisturbed-flow, the sinusoidal inflow, and the gust-counteracting potential flow. At the NSP, the first of these vanishes, since NSP is a stagnation point of the undisturbed flow (Eq. (3-5)). The second contribution (the inflow sinusoidal gust) vanishes also since it is finite (small, actually) in the Z-plane (Eq. 3-10) and is annihilated by $dZ/d\zeta$ at the leading edge or NSP, in accordance with Eq. (3-9) and the remarks following that equation.

Without closer investigation, it would appear that the third contribution to q at the NSP would vanish for the same reason. However, as indicated earlier, this component (the counteracting flow) proves to be singular of just the correct strength (as $X \to -B$) as to offset the vanishing of $dZ/d\zeta$ and contribute to q at the physical NSP. We shall devote most of the remainder of the report to this computation.

The terms $\partial\phi/\partial t$ in Eq. (4-1) should be examined (as they may) in the Z plane. The contributions to $\partial\phi/\partial t$ on the right-hand side of Eq. (4-1) come from the inflow gust and the counteracting nonsteady flow. But the first of these is exactly balanced by the $\partial\phi/\partial t$ on the left-hand side. We are assuming here that the sinusoidal gust inflow can be described by a potential flow. This is not true of physical turbulance but it is sufficient for the present single-sinusoidal argument, and we can easily construct potential flows having the prescribed transverse form (3-10) on the X axis.

Thus all that survives of the $\partial\phi/\partial t$ terms on both sides of Eq. (4-1) is the contribution to the right hand side due to the gust-counteracting flow. It will turn out that this vanishes on the upstream X-axis right up to the leading edge and hence vanishes at the NSP in the physical plane. This will emerge from the gust-entry calculation but is actually a direct consequence of the fact that the Z-plane gust-entry ϕ-function is odd in Y, vanishing upstream of the slit and exhibiting an antisymmetric jump on and downstream of the slit. Since the jump in ϕ is regular (nonsingular at the leading edge) therefore ϕ and, with it $\partial\phi/\partial t$, vanishes at the NSP.

The consequence of the foregoing statements with respect to the pressure fluctuation at the NSP is as follows:

$$p - p_\infty \cong \frac{\rho_o}{2} (U_o^2 - q_1^2) \tag{4-3}$$

wherein q_1 is the velocity magnitude due to the gust-entry-counteracting potential flow in the Z plane, mapped to the NSP of the z plane. That is

$$q_1 = \mathcal{L}_{Z \to (-B, 0^{\pm})} [u(Z) - iv(Z)] \frac{\frac{dZ}{d\zeta}}{\frac{dz}{d\zeta}} \tag{4-4}$$

V. LIMITING BEHAVIOR OF VELOCITY TRANSFORMATION AT NSP

We examine in detail, in this section, the limiting behavior of the velocity transformation equation (3-9) as the NSP is approached in the physical plane or, what is equivalent,

$$\left.\begin{array}{l} \text{as} \quad Z \to (-B^{+},0) \\ \\ \text{or} \\ \qquad z \to (-\ell(1+2\epsilon)^{+},0) \end{array}\right\} \tag{5-1}$$

Inverting Eq. (2-8) we find

$$\left.\begin{array}{l} \zeta = -\ell\epsilon + Z + \sqrt{Z^2-B^2} \\ \\ \text{where} \quad B = \ell(1+\epsilon) \end{array}\right\} \tag{5-2}$$

We consider points $Z^{\pm}$ on the top and bottom, respectively, of the slit and accomplish the approach to the leading edge as follows: We let

$$Z^{\pm} = -B + r \Big|_{\substack{\text{top} \\ \text{bottom}}} \tag{5-3}$$

with r small with respect to $\epsilon\ell$ and positive, real.

$$r \ll \epsilon\ell \tag{5-4}$$

Then, from (5-2), corresponding points $\zeta^{\pm}$ are given by

$$\zeta^{\pm} = -\ell\epsilon - B + r \pm i\sqrt{2Br-r^2} \tag{5-5}$$

Then the denominator $dz/d\zeta = (1 - \frac{\ell^2}{\zeta^2})$ in Eq. (3-9) remains finite as $r \to o$.

$$\left.\frac{dz}{d\zeta}\right|_{r\to o} = 1 - \frac{\ell^2}{\ell^2(1+2\epsilon)^2} = 1 - \frac{1}{(1+2\epsilon)^2}$$

$$\cong 1 - [1-4\epsilon-4\epsilon^2+16\epsilon^2]$$

$$= 4\epsilon(1-3\epsilon)$$

(5-6)

Since our Z-plane gust-entry analysis will be good only to order ϵ, therefore we keep only terms to this order in Eq. (5-6) and write

$$\left.\frac{dz}{d\zeta}\right|_{r\to o} \cong 4\epsilon$$

(5-7)

The numerator $dZ/d\zeta$ in Eq. (3-9) is more involved. It can be written as

$$\frac{dZ^{\pm}}{d\zeta} = \left\{ 1 - \frac{B^2}{(\zeta+\ell\epsilon)^2} \right\}^{\pm}$$

$$= \left\{ 1 - \frac{B^2}{(Z + \sqrt{Z^2-B^2})^2} \right\}^{\pm}$$

$$= \left\{ 1 - \frac{B^2}{(+B-r \mp i\sqrt{2Br-r^2})^2} \right\}$$

(5-8)

This can be expanded to give

$$\frac{dz^{\pm}}{d\zeta} = \left\{ 1 - \frac{1}{\left(1- \frac{r}{B} \mp i\sqrt{2\frac{r}{B} - \frac{r^2}{B^2}}\right)^2} \right\}$$

$$\simeq \left\{ 1 - \frac{1}{\left(1- \frac{r}{B} \mp i\sqrt{\frac{2r}{B}}\left(1- \frac{r}{4B}\right)\right)^2} \right\}$$

$$\simeq \left\{ 1 - \frac{1}{\left(1 \mp 2i\sqrt{\frac{2r}{B}} - \frac{4r}{B} + O\left(\frac{r}{B}\right)^{3/2}\right)} \right\}$$

$$\simeq \left\{ 1 - \left(1 \pm 2i\sqrt{\frac{2r}{B}} + \frac{4r}{B} - \frac{8r}{B}\right) + O\left(\frac{r}{B}\right)^{3/2} \right\}$$

$$= \mp 2i\sqrt{\frac{2r}{B}} + \frac{4r}{B}$$

(5-9)

Keeping only terms of order $\sqrt{\frac{r}{B}}$, and utilizing results (5-6) and (5-9) in Eq. (3-9) we find

$$w(z)\Big|_{Z=(-B+r)_{\substack{\text{top}\\\text{bottom}}}} \cong w\Big(\underbrace{-B+r, 0^{\pm}}_{\text{in Z plane}}\Big) \frac{\left(\mp 2i\sqrt{\frac{2r}{B}}\right)}{4\epsilon} \tag{5-10}$$

Now $w = u - iv$, and the counteracting part of v simply cancels out the sinusoidal gust of Eq. (3-10), which is finite everywhere. Thus the v contribution to (5-10) is annihilated as $r \to 0$, i.e. as we approach the nose or NSP in the physical plane.

However, the u-part of w on the slit is singular. In fact, foreseeing the form in which the result will emerge, we write

$$u(X, 0^{\pm}) = \pm \frac{1}{2}\sqrt{\frac{B-X}{B+X}}\, f(X,t) \tag{5-11}$$

where, in fact, f is regular for all X and depends harmonically on time t. We simply keep t as a parameter for the present. We will find the function f in the next section. However, we see that as

$$X \to (-B+r)$$

$$u(X,0^{\pm}) \to \pm \frac{1}{2}\sqrt{\frac{2B}{r}}\, f(-B,t) \tag{5-12}$$

Then, from Eq. (5-10)

$$w(z) \to \mp \frac{2i\sqrt{\frac{2r}{B}}}{4\epsilon}\left(\pm \frac{1}{2}\sqrt{\frac{2B}{r}}\right) f(-B,t)$$

or

$$u - iv \to -\frac{i}{2\epsilon} f(-B,t) \tag{5-13}$$

Since, physically, f must be real, we have

$$u \to 0$$

$$q \to v \to \frac{f(-B,t)}{2\epsilon} \tag{5-14}$$

as the NSP is approached (as $r \to 0$).

This is physically reasonable, since the vertical tangent at the nose (in the physical plane) prohibits any axial velocity u and permits only the vertical component v. We see, from Eq. (5-14), how the velocity induced at the NSP varies inversely with ϵ which, we recall, is 0.77 of the thickness-to-chord ratio.

The following section is devoted to the development, in detail, of the function f(X,t) first introduced in Eq. (5-11). In this development, the function sought will be the time-dependent vorticity density function $\gamma(X,t)$ which exists over the Z-plane slit and its wake (from +B to ∞) on the X axis. Eq. (5-11) is equivalent to foreseeing the form

$$\gamma\ (X,t) = \sqrt{\frac{B-X}{B+X}}\ f(X,t)$$

(5-15)

where vorticity and circulation are designated positive for a clockwise sense of rotation

and where f is real and everywhere regular.

It can be shown that the result of our double mapping procedure (Eq. (5-10)) for the transformation of the complex velocity in the nose region of the slit (Z) plane to that in the nose region of the physical (z) plane, agrees in magnitude with the correction factor of Lighthill's nonlinear theory for steady flow over lifting (asymmetric) airfoils. This follows from the fact, as pointed out by Van Dyke,[6] that the leading edge radius (a) of a Joukowski symmetric airfoil is given by

$$\begin{aligned} a &= 4\epsilon^2 \times \text{semichord} \\ &= 2\epsilon^2 \times \text{chord} \end{aligned} \qquad (5\text{-}16)$$

Then, as noted by Thwaites,[7] the first-order Lighthill correction for a two-dimensional profile of nose-radius (a) is achieved by multiplication of the linear-theoretical velocity by the factor

$$\sqrt{\frac{s}{s+\frac{a}{2}}}\ , \qquad (5\text{-}17)$$

where s is distance aft of the leading edge. In our notation, with

$$X = -B + r \tag{5-18}$$

it can be shown that

$$r = s + O(\epsilon \frac{r}{\ell}) + O(\epsilon^3) \tag{5-19}$$

Thus, as s→o the Lighthill correction factor approaches

$$\sqrt{\frac{s}{\frac{a}{2}}} \tag{5-20}$$

Our transformation factor in Eq. (5-10) is

$$\mp \frac{2i\sqrt{\frac{2r}{B}}}{4\epsilon} \simeq \mp \frac{i\sqrt{r}}{\sqrt{2}\ \epsilon\ \sqrt{\ell}}$$

$$\simeq \mp \frac{i\sqrt{r}}{\sqrt{2\epsilon^2 \ell}}$$

$$\simeq \mp \frac{i\sqrt{r}}{\sqrt{\epsilon 2 \cdot \text{chord}}}$$

$$\simeq \mp \frac{i\sqrt{r}}{\sqrt{\frac{a}{2}}} \simeq \mp \frac{i\sqrt{s}}{\sqrt{\frac{a}{2}}} \tag{5-21}$$

and this agrees, in magnitude, with Lighthill's result, Eq. (5-20). In Section VII herein, we use this agreement to generalize our results to shapes other than the Joukowski profile.

VI. THE GUST ENTRY PROBLEM IN THE Z-PLANE (DETAILS OF f(X,t))

Most of the analysis needed for the gust-entry problem for a flat plate is available in sources such as Reference 2. However, we depart slightly in some areas from the classical derivation to keep certain details clear and to focus attention on the results required for the present application.

The gust-counteracting flow in the Z plane is completely describable in terms of a time-dependent bound vorticity $\gamma_a(X,t)$ and a trailing or shed vorticity $\gamma_w(X,t)$, arising as a consequence of the time dependence of the total bound circulation $\Gamma(t)$.

$$\Gamma(t) = \int_{-B}^{B} \gamma_a(X,t)\, dX \tag{6-1}$$

Temporarily we admit complex time dependence $e^{i\omega_o t}$ (which leads to complex γ_a, γ_w) with the understanding that we will return to real quantities before involving the mapping from Z back to z. The inflow gust to be counteracted is given by (Eq. (3-10))

$$v = v_o\, e^{i(\omega_o t - k_o X)} \,. \tag{6-2}$$

Then our counteracting flow must be given by vorticity distributions γ_a, γ_w such that (dropping the $e^{i\omega t}$ time dependence which is common to v, γ_u, γ_w, and Γ)

$$-v_o e^{-i\frac{\omega_o X}{U_o}} = \frac{1}{2\pi}\int_{-B}^{B} \frac{\gamma_a(X')dX'}{X'-X} + \frac{1}{2\pi}\int_{B}^{\infty} \frac{\gamma_w(X')dX'}{X'-X} \,. \tag{6-3}$$

The assumption (3-10) that $v_o < \varepsilon U_o$ is what permits us to approximate the slightly wavy vortex wake geometry with the X-axis proper. It is one of the reasons why our gust-entry analysis is valid only to order ε, as was noted in Section V.

Scaling lengths with respect to B and using (temporarily)

$$\left.\begin{aligned} \frac{X'}{B} &= \xi \\ \frac{X}{B} &= x \end{aligned}\right\} . \tag{6-4}$$

and using the classical reduced frequency (corresponding to the slit in the Z-plane)

$$k = \frac{\omega_o B}{U_o} \tag{6-5}$$

we rewrite Eq. (6-3) in the scaled form

$$-v_o\, e^{-ikx} = \frac{1}{2\pi}\int_{-1}^{1} \frac{\tilde{\gamma}_a(\xi)d\xi}{\xi - x} + \frac{1}{2\pi}\int_{1}^{\infty} \frac{\tilde{\gamma}_w(\xi)d\xi}{\xi - x} \tag{6-6}$$

where $\tilde{\gamma}$ denotes γ in scaled variables $,x,\xi$.

Now the requirement of zero pressure jump across the wake demands that, in physical variables,

$$\gamma_w = \gamma_w(X - U_o t) \tag{6-7}$$

This, in turn, requires that

$$\gamma_w = e^{i\omega_o \left(t - \frac{(X-B)}{U_o}\right)} \gamma_w(B) \qquad (6\text{-}8)$$

or, in terms of scaled variables,

$$\tilde{\gamma}_w = e^{ik}\, e^{-ikx}\, \gamma_w(B) \qquad (6\text{-}9)$$

Then, vorticity conservation demands that

$$-\frac{d\Gamma}{dt} = \gamma_w(B)\,\frac{dX}{dt}$$

or

$$-i\omega_o\Gamma = U_o\,\gamma_w(B)$$

or

$$-\frac{ik\Gamma}{B} = \gamma_w(B) \qquad (6\text{-}10)$$

Thus

$$\tilde{\gamma}_w(x) = -\frac{ik\Gamma}{B}\, e^{ik}\, e^{-ikx} \qquad (6\text{-}11)$$

Reference (2) defines a convenient parameter Ω:

$$\Omega = \frac{\Gamma}{B}\, e^{ik} \qquad (6\text{-}12)$$

so that

$$\tilde{\gamma}_w(x) = -ik\,\Omega\, e^{-ikx} \qquad (6\text{-}13)$$

The value of Ω will be determined subsequently. Then Eq. (6-6) can be written

$$\frac{ik\Omega}{2\pi}\int_{1}^{\infty}\frac{e^{-ik\xi}}{\xi-x}\,d\xi - v_o\,e^{-ikx}$$

$$= \frac{1}{2\pi}\int_{-1}^{1}\frac{\tilde{\gamma}_a(\xi)d\xi}{\xi-x}$$

(6-14)

The inversion of this classical singular integral equation for $\tilde{\gamma}_a(\xi)$ is nonunique unless we invoke some additional requirement.[4] The Kutta condition is the appropriate one and, in the present context, takes the form of a boundedness requirement on $\gamma_a(\xi)$ at the trailing edge (ξ=1). With this condition, the inversion is rendered unique and takes the form[4]

$$\tilde{\gamma}_a(x) = -\frac{2}{\pi}\sqrt{\frac{1-x}{1+x}}\int_{-1}^{1}\sqrt{\frac{1+\xi}{1-\xi}}\,\frac{1}{\xi-x}\left\{ - v_o\,e^{-ik\xi}\right.$$

$$\left. + \frac{ik\Omega}{2\pi}\int_{1}^{\infty}\frac{e^{-ik\eta}d\eta}{\eta-\xi}\right\} d\xi$$

(6-15)

Because η varies over $(1,\infty)$ while ξ varies over $(-1,1)$, it is legal to invert the order of the ξ and η integrations (if they were in the same range this would not be legal but would require the use of the Poincare-Bertrand relation of singular integral equation theory).[4] Performing the inversion of order, we find

$$I = \int_{-1}^{1} \sqrt{\frac{1+\xi}{1-\xi}} \frac{d\xi}{(\xi-x)(\eta-\xi)} = \frac{1}{\eta-x} \int_{-1}^{1} \sqrt{\frac{1+\xi}{1-\xi}} \left(\frac{1}{\xi-x} - \frac{1}{\xi-\eta} \right) d\xi \tag{6-16}$$

We introduce the substitutions

$$\left.\begin{aligned} \xi &= \cos\theta \\ x &= \cos\varphi \\ \eta &= \cosh s \end{aligned}\right\} \tag{6-17}$$

Then Eq. (6-16) takes the form

$$I = \frac{1}{\eta-x} \int_{0}^{\pi} (1+\cos\theta) \left\{ \left(\frac{1}{\cos\theta-\cos\phi} \right) - \left(\frac{1}{\cos\theta-\cosh s} \right) \right\} d\theta \tag{6-18}$$

The first term gives[1]

$$\frac{\pi}{\eta-x} \tag{6-19}$$

while the second may be written as

$$
\begin{aligned}
&- \frac{1}{\eta - x} \int_0^{\pi} \frac{1 + \cos\theta - \cosh s + \cosh s}{\cos\theta - \cosh s}\, d\theta \\
&= - \frac{1}{\eta - x} \left\{ \pi + (1 + \cosh s) \int_0^{\pi} \frac{d\theta}{\cos\theta - \cosh s} \right\} \\
&= - \frac{1}{\eta - x} \left\{ \pi - (1 + \cosh s) \frac{\pi}{\sinh s} \right\}
\end{aligned}
\tag{6-20}
$$

as may be easily shown from integration by residues.

Thus, we find

$$
\begin{aligned}
I &= \frac{\pi}{\eta - x} \left(1 - 1 + \frac{1+\eta}{\sqrt{\eta^2 - 1}} \right) \\
&= \frac{\pi}{\eta - x} \sqrt{\frac{\eta+1}{\eta-1}}
\end{aligned}
\tag{6-21}
$$

Inserting this into Eq. (6-15) we find

$$
\begin{aligned}
\tilde{\gamma}_a(x) = - \frac{2}{\pi} \sqrt{\frac{1-x}{1+x}} \Bigg\{ & \int_{-1}^{1} \sqrt{\frac{1+\xi}{1-\xi}} \left(\frac{-v_o\, e^{-ik\xi}}{\xi - x} \right) d\xi \\
& + \frac{ik\Omega}{2} \int_1^{\infty} e^{-ik\eta} \frac{1}{\eta - x} \sqrt{\frac{\eta+1}{\eta-1}}\, d\eta \Bigg\}
\end{aligned}
\tag{6-22}
$$

Now, by definition

$$\Omega = \frac{\Gamma}{B} e^{ik} = \frac{e^{ik}}{B} \int_{-B}^{B} \gamma_w(X')dX' = e^{ik} \int_{-1}^{1} \tilde{\gamma}_w(\xi)\, d\xi \tag{6-23}$$

Thus we find Ω by operating on both sides of Eq. (6-22) with

$$e^{ik} \int_{-1}^{1} (\quad)\, dx \tag{6-24}$$

This gives, upon inverting integration orders, as we may,

$$\Omega = -\frac{2}{\pi} e^{ik} \int_{-1}^{1} \sqrt{\frac{1+\xi}{1-\xi}} \left(-v_o e^{-ik\xi}\right) \int_{-1}^{1} \sqrt{\frac{1-x}{1+x}}\, \frac{dx}{\xi-x}\, d\xi$$

$$-\frac{2}{\pi}(e^{ik})\frac{ik\Omega}{2} \int_{1}^{\infty} e^{-ik\eta} \sqrt{\frac{\eta+1}{\eta-1}} \int_{-1}^{1} \sqrt{\frac{1-x}{1+x}}\, \frac{dx}{\eta-x}\, d\eta \tag{6-25}$$

The first inner integral gives

$$\int_{-1}^{1} \sqrt{\frac{1-x}{1+x}}\, \frac{dx}{\xi-x} = \pi \tag{6-26}$$

while the second inner integral gives

$$\int_{-1}^{1} \sqrt{\frac{1-x}{1+x}}\,\frac{dx}{\eta-x} = \int_{o}^{\pi} \frac{(1-\cos\theta)d\theta}{\cosh s-\cos\theta} = \int_{o}^{\pi} \frac{1-\cos\theta+\cosh s-\cosh s}{\cosh s-\cos\theta}\,d\theta$$

or

$$\int_{-1}^{1} \sqrt{\frac{1-x}{1+x}}\,\frac{dx}{\eta-x} = \pi + (1-\cosh s)\,\frac{\pi}{\sinh s}$$

$$= \pi - \pi\sqrt{\frac{\eta-1}{\eta+1}} \qquad (6\text{-}27)$$

Thus

$$\Omega = -2\,e^{ik} \int_{-1}^{1} \sqrt{\frac{1+\xi}{1-\xi}}\,(-v_o\,e^{-ik\xi})\,d\xi$$

$$-2\,e^{ik}\,\frac{ik\Omega}{2} \int_{1}^{\infty} e^{-ik\eta}\sqrt{\frac{\eta+1}{\eta-1}}\left(1-\sqrt{\frac{\eta-1}{\eta+1}}\right)d\eta \qquad (6\text{-}28)$$

The second integral is, according to Ref. (2),

$$\int_{1}^{\infty} e^{-ik\eta}\left(\sqrt{\frac{\eta+1}{\eta-1}}-1\right)d\eta = -\frac{\pi}{2}\left\{H_1^{(2)}(k) + i\,H_o^{(2)}(k)\right\} - \frac{e^{-ik}}{ik} \qquad (6\text{-}29)$$

giving the result

$$\Omega\left[1-\frac{\pi}{2}\left[H_1^{(2)}(k)+i\,H_o^{(2)}(k)\right]ike^{ik}-1\right] = -2e^{ik}\int_{-1}^{1}\sqrt{\frac{1+\xi}{1-\xi}}\,(-v_o e^{-ik\xi})d\xi$$

or

$$\Omega = \frac{4}{\pi ik}\,\frac{\int_{-1}^{1}\sqrt{\frac{1+\xi}{1-\xi}}\,(-v_o e^{-ik\xi})\,d\xi}{\left[H_1^{(2)}(k)+i\,H_o^{(2)}(k)\right]} \qquad (6\text{-}30)$$

Most of the relations developed in this section thus far can be found directly in or inferred from the flat-plate gust entry theory presented in Reference (2). They are presented here primarily to make the present report self-contained.

Comparing the form of Eq. (5-15) for $\gamma(X,t)$ with the results of this section (Eq. (6-22) together with Eq. (6-30) for Ω) we see that the regular function $f(X,t)$ is given on the wing $(-B,B)$ by

$$\frac{f(X,t)}{e^{i\omega t}} = -\frac{2}{\pi}\left\{\int_{-B}^{B}\sqrt{\frac{B+X'}{B-X'}}\left(-\frac{v_o e^{-ikX'/B}}{X'-X}\right)dX' + \frac{ik\Omega}{2}\int_{B}^{\infty}\frac{e^{-ikX'/B}}{X'-X}\sqrt{\frac{X'+B}{X'-B}}\,dX'\right\} \qquad (6\text{-}31)$$

with Ω given by (6-30).

But all we need for the present application (Eq. (5-14)) is f(-B,t). For this we can use (6-31) with X set equal to -B.

Thus

$$\frac{f(-B,t)}{e^{i\omega t}} = -\frac{2}{\pi}\int_{-1}^{1}\sqrt{\frac{1+\xi}{1-\xi}}\left(-\frac{v_o e^{-ik\xi}}{\xi+1}\right)d\xi$$

$$-\frac{2}{\pi}\,\frac{ik\Omega}{2}\int_{1}^{\infty}\frac{e^{-ik\xi}}{\xi+1}\sqrt{\frac{\xi+1}{\xi-1}}\,d\xi$$

$$= +\frac{2}{\pi}\int_{-1}^{1}\frac{v_o e^{-ik\xi}}{\sqrt{1-\xi^2}}\,d\xi$$

$$-\frac{ik\Omega}{\pi}\int_{-1}^{\infty}\frac{e^{-ik\xi}}{\sqrt{\xi^2-1}}\,d\xi \qquad (6\text{-}32)$$

The first integral in (6-32) gives[3]

$$\frac{2}{\pi}\int_{-1}^{1}\frac{v_o e^{-ik\xi}}{\sqrt{1-\xi^2}}\,d\xi = \frac{1}{\pi}\int_{o}^{2\pi} v_o e^{-ik\cos\theta}\,d\theta$$

$$= 2\,v_o\,J_o(k) \qquad (6\text{-}33)$$

The second integral in (6-32) gives[3]

$$-\frac{1k\Omega}{\pi}\int_{1}^{\infty}\frac{e^{-ik\xi}}{\sqrt{\xi^2-1}}\,d\xi = -\frac{ik\Omega}{\pi}\,\frac{\pi}{2}\left(-i\,H_o^{(2)}(k)\right)$$

$$= -\frac{k\Omega}{2}\,H_o^{(2)}(k) \qquad (6\text{-}34)$$

Thus

$$\frac{f(-B,t)}{e^{i\omega t}} = 2v_o J_o(k) - \frac{k\Omega}{2}\,H_o^{(2)}(k) \qquad (6\text{-}35)$$

The integral required in the expression for Ω (Eq. (6-30)) may be performed, with the result,[3]

$$\int_{-1}^{1} \sqrt{\frac{1+\xi}{1-\xi}}\,(-v_o e^{-ik\xi})\,d\xi = -\frac{v_o}{2}\int_{o}^{2\pi}(1+\cos\theta)\,e^{-ik\cos\theta}\,d\theta$$

$$= -\frac{v_o}{2}\cdot 2\pi\left(J_o(k) + i\,J_1(-k)\right)$$

$$= -\pi v_o\left(J_o(k) - i\,J_1(k)\right) \qquad (6\text{-}36)$$

Thus

$$\Omega = \frac{4}{ik}\,\frac{(-v_o)\left(J_o(k) - i\,J_1(k)\right)}{\left(H_1^{(2)}(k) + i\,H_o^{(2)}(k)\right)} \qquad (6\text{-}37$$

Finally, we find for f(-B,t), from (6-35)

$$f(-B,t) = e^{i\omega t}\left\{2\,v_o J_o(k) - \frac{kH_o^{(2)}(k)}{2}\cdot\frac{4i}{k}\,v_o\cdot\left(\frac{J_o(k)-iJ_i(k)}{H_1^{(2)}(k)+iH_o^{(2)}(k)}\right)\right\}$$

$$= e^{i\omega t} v_o \left\{ 2 J_o(k) - \frac{2(H_1^{(2)}+iH_o^{(2)}-H_1^{(2)})(J_o-iJ_1)}{(H_1^{(2)}+i H_o^{(2)})} \right\}$$

$$= e^{i\omega t} \cdot 2 v_o \left\{ i J_1(k) + \frac{H_1^{(2)}(k)(J_o(k)-iJ_1(k))}{H_1^{(2)}(k)+i H_o^{(2)}(k)} \right\}$$

(6-38)

Now the quantity

$$\frac{H_1^{(2)}(k)}{H_1^{(2)}(k)+ i H_o^{(2)}(k)}$$ is the famous complex

Theodorsen C(k) function of oscillatory thin-wing theory.[2]
Now

$$k = \frac{\omega_o B}{U_o} \simeq \frac{\omega_o c}{2U_o} = \frac{U_o k_o c}{2U_o}$$

or

$$k \simeq \frac{c}{2} \frac{2\pi}{\lambda_o} = \frac{\pi c}{\lambda_o} \qquad (6\text{-}39)$$

since $B \simeq \frac{c}{2}$.

Thus, for inflow gust forms having wavelength λ_o of the order of chord c, we are in the region where k is of the order of π, which is large in oscillatory aerodynamic theory. For such large k,

$$C(k) \cong 0.5 + i \times 0 = 0.5 \tag{6-40}$$

and f(-B,t) simplifies to

$$f(-B,t) \cong 2\, v_o\, e^{i\omega t}\left(iJ_1(k) + \frac{1}{2}\left(J_o(k) - iJ_1(k)\right)\right)$$

$$= v_o\, e^{i\omega t}\left(J_o(k) + iJ_1(k)\right) \tag{6-41}$$

If we make the further asymptotic approximation for the $J_o(k)$, $J_1(k)$ as well, (this is not as well justified with k of the order of π, but if anything it slightly underestimates the contribution considered) then

$$f(-B,t) \cong v_o\, e^{i\omega t}\left(\sqrt{\frac{2}{\pi k}}\right)\left(\cos\left(k - \frac{\pi}{4}\right) + i\sin\left(k - \frac{\pi}{4}\right)\right)$$

$$\cong v_o\, e^{i\left(\omega t + k - \frac{\pi}{4}\right)}\sqrt{\frac{2}{\pi k}} \tag{6-42}$$

Returning to real form and unscaled variables,

$$f(-B,t) \cong v_o \sqrt{\frac{2}{\pi\, k_o\, B}}\cos\left(\omega t + k_o\, B - \frac{\pi}{4}\right) \tag{6-43}$$

Inserting this into our relation (5-14) for q_1 at the NSP in the physical plane

$$q_1 \tilde{=} \frac{v_o}{2\epsilon} \sqrt{\frac{2}{\pi k_o B}} \cos(\omega t + k_o B - \frac{\pi}{4}) \qquad (6\text{-}44)$$

For the case where encountered fluctuating scales are markedly larger than the chord length of the penetrating airfoil then the simple asymptotic-approximation form (Eq. (6-44)) for q_1 should be replaced by the more accurate relation arising from Eqs. (5-14) and (6-38); namely,

$$q_1 = \frac{2v_o}{2\epsilon} \, Re \left\{ e^{i\omega t} \left(i J_1(k) + \frac{H_1^{(2)}(k) \left(J_o(k) - i J_1(k)\right)}{H_1^{(2)}(k) + i H_o^{(2)}(k)} \right) \right\} \qquad (6\text{-}45)$$

The approximation

$$C(k) = \frac{H_1^{(2)}}{H_1^{(2)} + i H_o^{(2)}} \tilde{=} 0.5 + i (o)$$

is quite good for k values as small as 1.0.

The asymptotic approximations to J_o and J_1, however, should be replaced by their actual respective values for situations in which encountered fluctuation scales far exceed the penetrating airfoil chord length and k is, accordingly, less than π.

In support of our statement, in Section IV, concerning the vanishing of $\partial\phi/\partial t$ at the NSP, we note that the complex potential function for our gust-counteracting flow is given by

$$F(Z) = \varphi + i \psi = \frac{i}{2\pi} \int_{-B}^{\infty} \gamma(X') \, Ln(Z - X') \, dX' \qquad (6\text{-}46)$$

For real (physical) $\gamma(X,t)$ this gives

$$\varphi = -\frac{1}{2\pi} \int_{-B}^{\infty} \gamma(X',t) \tan^{-1} \frac{Y}{X-X'} \, dX' \qquad (6\text{-}47)$$

and we see that ϕ and $\partial\phi/\partial t$ are odd in Y and therefore vanish on the X axis upstream of X=-B. Since the jump in ϕ across the airfoil is not singular, in contrast to $\gamma(X,t)$, therefore ϕ and $\partial\phi/\partial t$ vanish at the nose (X=-B) and therefore vanish at the NSP in the physical plane as well.

Thus we have finally for the fluctuating pressure at the NSP in the physical plane

$$p - p_\infty = \frac{\rho_o}{2} \left(U_o^2 - \frac{v_o^2 \cos^2(\omega t + k_o B - \frac{\pi}{4})}{2\epsilon^2 \pi k_o B} \right) \qquad (6\text{-}48)$$

VII. COMPARISON OF PRESSURE FLUCTUATIONS INDUCED BY TRANSVERSE AND LONGITUDINAL VELOCITY FLUCTUATIONS

As an approximate measure of the effect of pressure fluctuations induced by axial velocity fluctuations

$$u = U_o + \delta u \cos(\omega_o t - k_o x) \tag{7-1}$$

we simply take the quasi-steady result *

$$\delta p \Big|_{\text{due to } \delta u} \sim - \rho_o U_o \delta u \tag{7-2}$$

Assuming δu of the same order as v_o (isotropy in planes normal to the wing span) we see that the ratio μ of pressure fluctuation amplitudes induced by transverse velocity fluctuations to those induced by axial fluctuations is given approximately by

$$\mu \simeq \frac{v_o}{4 \epsilon^2 \pi U_o k_o B} = \frac{v_o \lambda_o}{8 \epsilon^2 \pi^2 B U_o} \tag{7-3}$$

Recalling that $\epsilon = \frac{4}{3\sqrt{3}} \times \frac{\text{thickness}}{\text{chord}}$,

$$\mu \simeq \frac{v_o}{U_o} \frac{\lambda_o}{B} \frac{1}{8\pi^2} \times \frac{27}{16} \left(\frac{\text{chord}}{\text{thickness}} \right)^2 \tag{7-4}$$

Since $B \simeq \frac{1}{2}$ chord, this is equivalent to

*In fact, Bearman's experimental results[5] with a bluff body show this to be satisfied within 5% for scales λ_o more than five times as big as body thickness, and we are restricting our treatment to this regime.

$$\mu \cong \frac{v_o}{U_o} \frac{\lambda_o}{\text{thickness}} \frac{\text{chord}}{\text{thickness}} \frac{27}{64\ \pi^2}$$

$$\cong \frac{1}{23} \left\{ \frac{v_o}{U_o} \frac{\lambda_o}{\text{thickness}} \frac{\text{chord}}{\text{thickness}} \right\} \qquad (7\text{-}5)$$

This makes clear what is required to give physical significance to the transverse-gust-induced contribution to pressure fluctuations; namely large $\frac{\lambda_o}{\text{thickness}}$, large $\frac{\text{chord}}{\text{thickness}}$ and slow penetration velocity U_o or strong fluctuation intensity (v_o).

If $\lambda_o \sim$ chord

and $\frac{\text{chord}}{\text{thickness}} \sim 10$

Then $$\mu \cong \frac{100}{23} \frac{v_o}{U_o} \ . \qquad (7\text{-}6)$$

Thus for $\frac{v_o}{U_o} \sim 1\%$, $\mu \sim \frac{1}{23}$

while for $\frac{v_o}{U_o} \sim 10\%$, $\mu \sim \frac{1}{2.3}$ (7-7)

We should now be able to remove any restriction implicit in our use of a Joukowski profile by replacing the ϵ^2, which appears in expression (7-3) for μ, by the relation (Eq. (5-16)) between ϵ^2 and nose-radius (a)

$$\epsilon^2 = \frac{a}{2 \times \text{chord}} \qquad (7\text{-}8)$$

Then, in accord with the Lighthill theory,[7] we can write our ratio μ in terms of profile nose radius and thereby add generality

to the result. Thus, in terms of nose radius, for any symmetric profile of small thickness-to-chord ratio,

$$\mu \cong \frac{v_o \lambda_o}{4 \frac{a}{\text{chord}} \pi^2 B U_o}$$

$$\cong \frac{v_o \lambda_o}{2a \pi^2 U_o} \quad \text{since } B \cong \frac{c}{2}$$

$$= \frac{1}{2\pi^2} \frac{v_o}{U_o} \frac{\lambda_o}{a}$$

$$\cong \frac{1}{20} \frac{v_o}{U_o} \frac{\lambda_o}{\text{nose radius}} \qquad (7\text{-}9)$$

This expresses the relative importance of transverse and axial fluctuation velocity components, in affecting NSP pressure fluctuations, directly in terms of the ratios of $\frac{\text{fluctuation velocity}}{\text{penetration velocity}}$ and $\frac{\text{fluctuation scale}}{\text{nose radius}}$.

For a profile whose nose region resembles that of a symmetric Joukowski profile, expressions (7-9) and (7-5) should agree. If the nose region of the profile of interest differs markedly from the Joukowski nose profile, then relation (7-9) should still be valid.

VIII. CONCLUSIONS

The results of our analysis relating NSP pressure fluctuations to encountered velocity fluctuations are contained in expressions (6-48), (7-5), and (7-9). We reiterate that the present analysis applies only to fluctuation scales which are large relative to profile thickness. They may, however, be of the same order as profile chord-length. The aforementioned results indicate that as the ratios

$$\frac{\text{fluctuation scale}}{\text{nose radius}} = \frac{\lambda_o}{a}$$

and

$$\frac{\text{fluctuation velocity}}{\text{penetration velocity}} = \frac{v_o}{U_o}$$

increase such that their product approaches a number of the order of 20, then transverse velocity fluctuations become as important as axial fluctuations. For fluctuation scales whose length is at least an order of magnitude less than the profile chord, Bearman's results[5] should serve to relate NSP pressure fluctuations to encountered axial velocity fluctuations. For fluctuation scales of the order of profile chord or longer, Bearman's results probably still apply if conditions are such that our transverse velocity effectiveness ratio μ is still small. This would require verification. When μ is not small, then Bearman's results cannot be used, since they neglect the effects of transverse velocity altogether.

When conditions are such that μ is large, then the transverse velocity fluctuations dominate the fluctuation pressure at the NSP, and our expression (6-48) gives the result. As in Section VII herein, we can add generality to Eq. (6-48) (which was derived for a Joukowski profile) by replacing ϵ therein with

$$\epsilon = \sqrt{\frac{a}{2 \times \text{chord}}} \qquad (8\text{-}1)$$

With this substitution our expression (6-48) should give the pressure at the NSP, valid for the large-μ regime, for nose shapes more general than that characterizing the Joukowski profile.

For the case where μ is large and the encountered fluctuation scales are large with respect to penetrating airfoil chord length, then the approximate Eq. (6-44) for q_1 should be replaced by the more accurate expression (6-45) in forming the fluctuation

pressure at the NSP. Equation (8-1), replacing ε by its equivalent in terms of nose-radius, can still be used within this improved relation (6-45) to remove any restrictions imposed by the assumption of a Joukowski profile.

REFERENCES

1. Glauert, H., The Elements of Aerofoil and Airscrew Theory, Second Edition, University Press, Cambridge, (1947).

2. Bisplinghoff, R. L., Ashley, H. and Halfman, R. L., Aeroelasticity, Addison-Wesley Publishing Co., Inc., Reading, Massachusetts, (1955).

3. McLachlan, N. W., Bessel Functions for Engineers, Second Edition, Clarendon Press, Oxford, (1955).

4. Course Lecture Notes; "Singular Integral Equation Theory," Professor Arthur S. Peters, Courant Institute, New York University, Spring Term, 1955.

5. Bearman, P. W., "Some Measurements of the Distortion of Turbulence Approaching a Two-Dimensional Bluff Body," J. Fluid Mech., vol. 53, part 3, pp. 451-467, 1972.

6. Van Dyke, Milton, Perturbation Methods in Fluid Mechanics, Academic Press, New York and London, (1964).

7. Fluid Motion Memoirs, INCOMPRESSIBLE AERODYNAMICS, Ed. Bryan Thwaites, Clarendon Press, Oxford, (1960).